Mechanisms of ultrafast laser-induced deep-subwavelength gratings on graphite and diamond

Min Huang,[1,*] Fuli Zhao,[1] Ya Cheng,[2] Ningsheng Xu,[1] and Zhizhan Xu[2,†]
[1]*State Key Laboratory of Optoelectronic Materials and Technologies, Sun Yat-sen University, Guangzhou 510275, China*
[2]*State Key Laboratory of High Field Laser Physics, Shanghai Institute of Optics and Fine Mechanics, Chinese Academy of Sciences, P.O. Box 800-211, Shanghai 201800, China*
(Received 18 December 2008; revised manuscript received 4 February 2009; published 30 March 2009)

Deep-subwavelength gratings with periodicities of 170, 120, and 70 nm can be observed on highly oriented pyrolytic graphite irradiated by a femtosecond (fs) laser at 800 nm. Under picosecond laser irradiation, such gratings likewise can be produced. Interestingly, the 170-nm grating is also observed on single-crystal diamond irradiated by the 800-nm fs laser. In our opinion, the optical properties of the high-excited state of material surface play a key role for the formation of the deep-subwavelength gratings. The numerical simulations of the graphite deep-subwavelength grating at normal and high-excited states confirm that in the groove the light intensity can be extraordinarily enhanced via cavity-mode excitation in the condition of transverse-magnetic wave irradiation with near-ablation-threshold fluences. This field enhancement of polarization sensitiveness in deep-subwavelength apertures acts as an important feedback mechanism for the growth and polarization dependence of the deep-subwavelength gratings. In addition, we suggest that surface plasmons are responsible for the formation of seed deep-subwavelength apertures with a particular periodicity and the initial polarization dependence. Finally, we propose that the nanoscale Coulomb explosion occurring in the groove is responsible for the ultrafast nonthermal ablation mechanism.

DOI: 10.1103/PhysRevB.79.125436 PACS number(s): 78.66.Tr, 78.47.−p, 79.20.Ds, 81.16.Rf

I. INTRODUCTION

In laser ablation, a universal phenomenon is the appearance of laser-induced periodic surface structure.[1–5] It is generally accepted that the classic ripples, which always exhibit the characteristic periodicity close to the laser wavelength, arises from the interference of incident laser with scattering waves from surface roughness.[2–5] In recent decade, as femtosecond (fs) laser is widely used in the field, a new kind ripple with the periodicity significantly smaller than the laser wavelength is observed.[6–27] The morphological characteristic of such a novel deep-subwavelength ripple resembling the grating fabricated by advanced micro/nanofabrication technologies is greatly different from that of classic ripples which always have smooth profiles.[17,24–26] In addition, the reported periodicities of such gratinglike structures, which vary from one half to tenth of laser wavelength, and the strict polarization dependence of the grating orientation cannot be deduced from the classic scattering wave model.[9] By far, some theoretical models for qualitative description of the phenomena have been proposed, whereas the origin of the deep-subwavelength gratings (for brevity, the deep-subwavelength grating is called as nanograting[17,25] in the following) is still not very clear. The periodicities of the nanogratings cannot be derived quantificationally; the main causes of the distinct polarization dependence of grating orientation are still ambiguous.

Recently, the extraordinary transmission phenomenon through subwavelength structure has given rise to considerable interest[28–34] because it shows that orders of magnitude more light than prediction can be transmitted through the structure. In general, these investigations are focused on metallic films, which can offer free electrons to excite surface plasmons (SPs) for generating extraordinarily enhanced transmission.[28–32] In addition, for one-dimensional grating, the cavity(waveguide)-mode excitation is important for the enhancement.[31–34] At first glance, this phenomenon appears to bear no relation to the laser-induced nanogratings, which are apt to appear on dielectric or semiconductor rather than on metal. Nevertheless, actually, such nanogratings have a similar morphological characteristic of the gratings fabricated by other nanomachining technologies for enhanced transmission. Therefore, we can expect light enhancement in the groove under laser irradiation. In addition, as is well known that high fluence irradiation can excite abundant free electrons and form plasma on dielectric surface or in dielectric,[35–39] which exhibits metallic characteristic, we can further expect extraordinary light enhancement in nanoapertures of dielectric surface under such an irradiation condition via the excitation of SPs or cavity mode such as the cases in metallic film. In short, we propose that the optical properties of nanogratings on nonmetallic materials irradiated by ultrafast laser pulses with a fluence near the ablation threshold resemble that on metallic film irradiated by a low fluence light.

Nowadays, we have carried out ablation experiments on graphite and diamond and observed nanogratings on the ablated areas with similar topographies and periodicities. The phenomenon that nanogratings can appear on opaque graphite by fs and picosecond (ps) laser irradiations is interesting and significant. Moreover, the similarity of the nanogratings on graphite and diamond can give us new insights to the exact physical mechanisms of nanograting formation and promote our understanding of ultrafast interactions.

In the following, we first introduce the experimental details in Sec. II and then demonstrate the experimental results of laser-induced nanogratings on graphite as well as diamond in Sec. III. Based on these results, in Sec. IV, we give some simulations about the optical properties of the nanograting at normal and high-excited states and discuss the mechanism of extraordinary light enhancement via cavity-mode excitation,

which acts as an important feedback mechanism for the growth and polarization dependence of nanogratings. Furthermore, in Sec. V, we discuss the two main origins for the polarization dependence of nanogratings in detail, talk of the effect of surface roughness on nanograting formation, and at last describe the picture of nanoscale Coulomb explosion (CE) occurring in the groove, which is responsible for the ultrafast nonthermal ablation mechanism.

II. EXPERIMENTAL DETAILS

A highly oriented pyrolytic graphite (HOPG) sample (SPI Supplies, Grade SPI-II) with dimensions of $10 \times 10 \times 1$ mm^3 and a natural single-crystal bulk diamond sample (De Beers Diamond Corporation) with optical surface polishing were used in this study. Note that HOPG is not a single crystal but has an extremely high degree of *c*-axis orientation of small graphite crystals along the normal of the flake. As is well known, graphite has physical properties of high anisotropy, such as the high conductivity in the *a*-*b* plane and the low conductivity in the *c*-axis direction.

A regenerative Ti:sapphire oscillator-amplifier system (Spectra Physics Hurricane) based on the chirped-pulsed amplification (CPA) technique at a central wavelength of 800 nm with pulse duration of 125 fs and repetition rate of 1 kHz was used to perform fs ablation experiments. 400-nm-fs pulses were obtained by frequency doubling with a KDP crystal (1 mm thick). A mode-locked Nd:YAG laser (EKSPLA, PL2143B) with pulse duration of 30 ps and repetition rate of 10 Hz was used for implementing ps experiments. The ps pulses of different wavelengths were obtained by the optical parametric generators (EKSPLA, PG411/511) pumped with the Nd:YAG laser. A variable neutral density filter was utilized to adjust the pulse energy for approaching the ablation threshold. Then the linearly polarized Gaussian laser beam was focused with a convex lens (Newport, UV fused silica precision planoconvex lens; focal length 300 mm). The samples were mounted on an electric *XYZ*-translation stage and observed real time by a charge-coupled device (CCD) monitor equipped with an objective lens of long focus. The number of laser pulses imposed per site on sample surface was determined by an electric shutter, which can control the irradiation time of laser pulses with definite repetition rate. All experiments were performed in an ambient air with sample surface perpendicular to the direction of laser beam propagation. The ablation spots were analyzed with scanning electron microscopy [(SEM) JEOL JSM-6380 and Quanta 400F].

III. EXPERIMENTAL RESULTS

A. Nanogratings on graphite

Figure 1(a) shows the SEM images of graphite surface irradiated by 3000 fs pulses of 800 nm with a fluence of 0.17 J/cm^2, which is near the ablation threshold of graphite. Therefore, the ablation rate is very low, as demonstrated by the complanate profile of the whole ablation crater. It is obvious that the nanograting with the periodicity about 180 nm and orientation perpendicular to the laser polarization covers the ablated area with few redeposited materials, demonstrating little collateral thermal effect. The profile of the nanograting, exhibiting a wide planar ridge and a narrow groove with very sharp brinks in a period, differs greatly from that

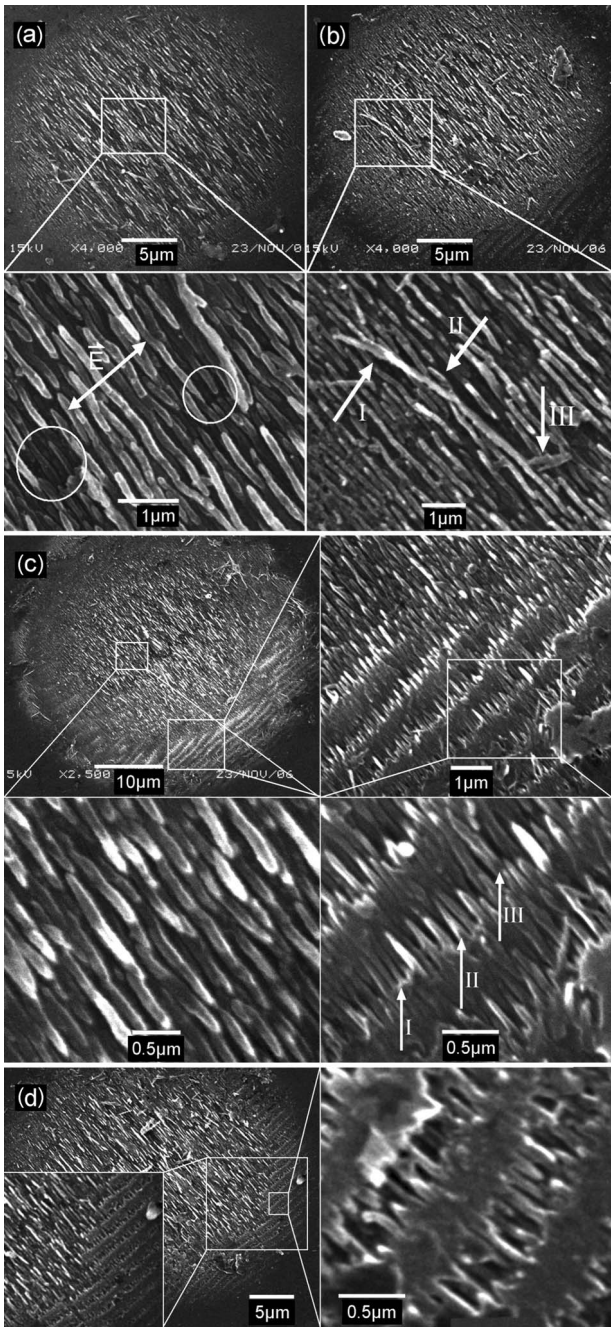

FIG. 1. SEM images of graphite surface irradiated by 800-nm fs laser with a fluence of 0.17 J/cm^2 and different pulse numbers. (a) 3000 pulses. Double arrow: the polarization of incident laser. Circles: the low-lying regions with ridges broken off. (b) 1000 pulses. Arrow I: a ridge with a length of about 8 μm partially broken off its original location. Arrow II: the original location of the ridge. Arrow III: a thin sheet. (c) 100 000 pulses. Arrow I, II, and III denote nanogratings with periodicities of 70, 120, and 170 nm, respectively. (d) 10 000 pulses. The fine nanograting of 120 nm independently appears in the classic ripple areas.

of classic ripples with smooth surface envelop and indicates distinct physical mechanisms.

In detail, the surface topography is not absolute even: some regions are depressed with low-lying ridges, as denoted by the circles in Fig. 1(a). It appears that a part of the ridges have broken off these regions. As shown in Fig. 1(b), an 8-μm ridge has partially broken off its original location and some thin sheets which look like the debris of the sheddings distribute randomly. It seems that a strong localized shock exists in the grooves during ablation and causes the ridge shedding.

With pulse number being very large, an interesting phenomenon can be observed—the periodicity at the brim may be different from that in the central area. As shown in Fig. 1(c), at the brim the nanogratings modulated by classic ripples appear with periodicities of 170, 120, and 70 nm. The minimum periodicity is only 1/11 of the laser wavelength. Considering the facts that the periodicity 170 nm remains almost unchanged in various craters ablated with pulse numbers in a wide range and the simultaneous appearance of three different periodicities in one crater, we can conclude that the 120-nm and 70-nm gratings should not evolve from the 170-nm grating via gradual decrease in periodicity along with the increase in pulse number. In other words, it is plausible to suggest that the periodicities of 170, 120, and 70 nm are all the viable periodicities of nanogratings on graphite. This proposition is further confirmed by Fig. 1(d), which demonstrates that the 120-nm grating independently appears in the classic ripple area. The occurrence of simultaneous multiperiodicities for deep-subwavelength ripples is an interesting property for nanogratings on graphite, which is somewhat similar to certain results reported in Refs. 10 and 21.

With the ps laser irradiation, such nanogratings can also be formed. As shown in Fig. 2(a), the nanogratings of 130 and 80 nm can be observed on the wall of the crater ablated by the 532-nm ps laser. Although the nanogratings tend to be produced by fs laser multiphoton irradiation,[11] lately the nanogratings induced by ps laser have also been reported.[22–24] Our results of nanogratings produced by the 30-ps laser on opaque graphite further confirm that the pulse duration of fs time scale is an appropriate condition rather than the necessary condition for nanograting formation.

Note that the nanogratings of 130 and 80 nm induced by the 532-nm laser should correspond to the gratings of 170 and 120 nm rather than 120 and 70 nm induced by the 800-nm laser, respectively. In other to confirm this, we have carried out ablation experiments with different laser wavelengths. In a wide wavelength range [the cases of 400-nm and 1300-nm wavelengths are shown in Figs. 2(b) and 2(c), respectively], the coarse nanograting (the 170-nm grating at 800-nm wavelength is ascribed to) can be easily observed. The linear relationship between the laser wavelength and the periodicity of coarse nanograting is shown in Fig. 2(d), which resembles the result on ZnO.[24]

B. Nanogratings on diamond

The surface morphology of diamond irradiated by the 800-nm fs laser is demonstrated in Fig. 3. For the fluence

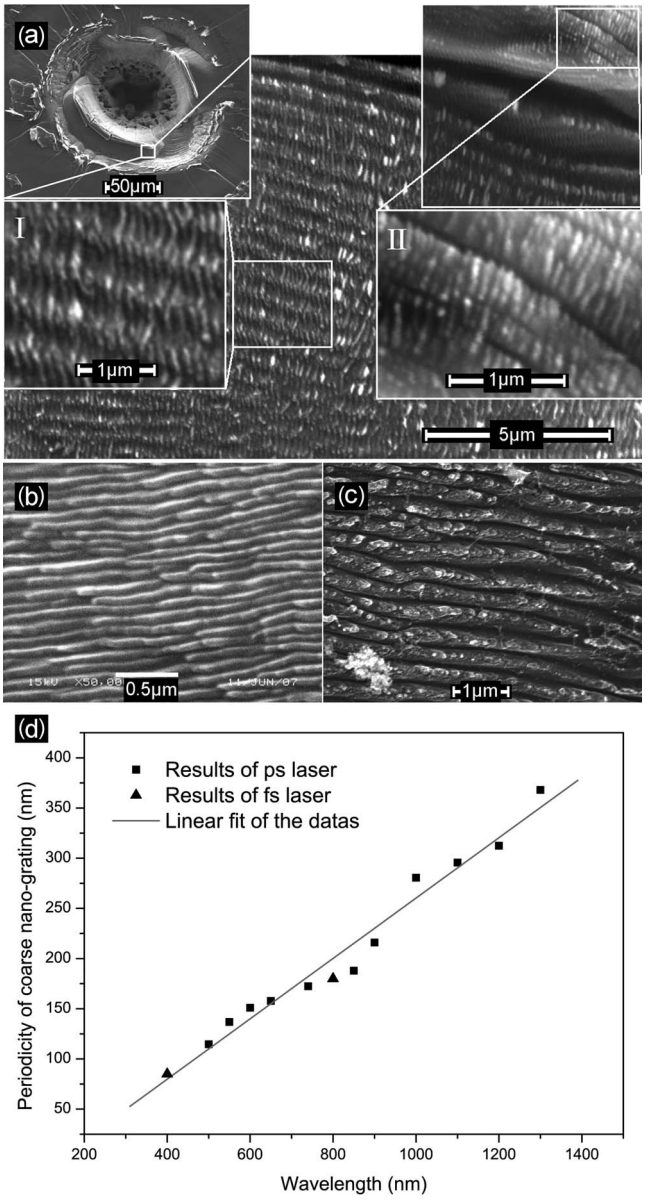

FIG. 2. Nanograting characteristics of graphite surface irradiated by lasers with different pulse durations and wavelengths. (a) SEM image of graphite surface irradiated by 532-nm ps laser with 2000 pulses at a fluence of 46 J/cm^2. Area I and II show nanogratings with periodicities of 130 and 80 nm, respectively. (b) SEM image of graphite surface irradiated by 400-nm fs laser with 50 000 pulses. (c) SEM image of graphite surface irradiated by 1300-nm ps laser with 300 pulses. (d) The relationship between the laser wavelength and the periodicity of coarse nanograting.

near the ablation threshold [Fig. 3(a)], in the whole ablation area, a quite regular nanograting with abrupt verges between ridges and grooves appears with a periodicity of 170 nm. At a slightly higher fluence [Fig. 3(b)], the orderly grating near the crater center is somewhat different from that at the brim. The grating profile is smoother and the periodicity of 190 nm is larger than the periodicity of 170 nm at the brim due to stronger thermal effect. At the outmost brim, an ultraregular nanograting with groove terminal size of about 10 nm can be observed. Comparing Fig. 3 with Fig. 1, we can see that the

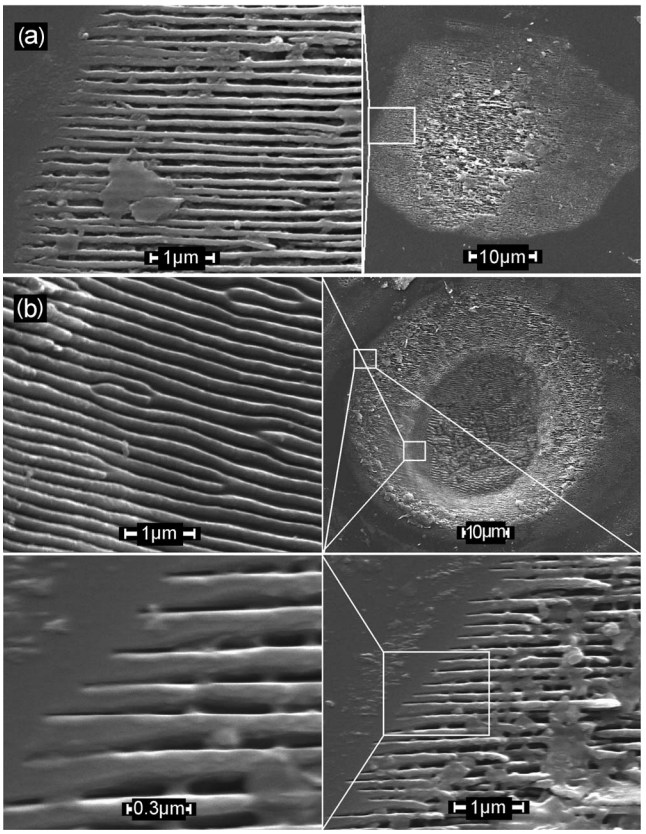

FIG. 3. SEM images of diamond surface irradiated by 800-nm fs laser with different fluences and pulse numbers. (a) 3000 pulses at a fluence of 1.9 J/cm^2. At the brim, the nanograting with a periodicity of 170 nm appears in accurate order. (b) 8000 pulses at a fluence of 2.8 J/cm^2. The nanogratings at the wall and the brim of the crater with periodicities of 190 and 170 nm, respectively, are both highly regular.

nanogratings formed on the two carbon allotropes have similar morphological characteristics—identical periodicity and grating features, which imply that the dynamic process of nanograting formation on these carbon allotropes is the same. In fact, in view of the similar laser-induced nanoripples on diamondlike carbon (DLC) film,[12,13,21] a further universality for the above-mentioned proposition can be obtained.

C. Some insights

Summing up the experimental results, we can see that the formation of nanogratings on graphite and diamond under ultrafast laser irradiation with near-threshold fluences is a universal phenomenon. These results are significant for the understanding of the formation mechanism of various laser-induced nanogratings, as it can give us some insights for laser-matter interactions. First, the nanogratings formed on graphite that is opaque definitely demonstrate that the one-photon transparency is not the necessary condition for that. Actually, the fs laser-induced nanoripples with periodicities far smaller than laser wavelengths on Si,[10,14,19] InP,[18] and Cu,[23] which are all opaque to the respective incident lasers, likewise approve the conclusion. It implies that ultrafast laser-induced deep-subwavelength ripple is a universal phenomenon in laser-solid-matter interaction, which should relate to some basic physical processes and mechanisms. Second, the appearance of simultaneous ultrafine nanogratings with different periodicities shows that the periodicity is not always singleness and implies the fluence effect (at the brim the fluence is low), certain resonant characteristics, or self-organization characteristic.[10] Third, from the morphologies of nanogratings on graphite and diamond, it can be seen that the nanogratings are formed on intrinsic surface rather than on amorphous carbon layer induced by thermal effects. This conclusion is further confirmed by micro-Raman spectrum results,[40] which reveal that nanograting areas maintain mainly bulk crystal structures covered by an ultrathin amorphous layer (similar to the structural character of that on ZnO reported in Ref. 24). Thus, an ultrafast nonthermal mechanism should be responsible for the nanograting formation. Fourth, as is well known, at normal-state graphite and diamond have very different physical properties, especially the optical property—one opaque, the other transparent. Considering these facts and the resemblance of nanogratings on graphite and diamond, we can conclude that the formation of nanograting is not determined by the physical properties of materials at normal states, i.e., we should consider the high-excited states of materials for these problems.

IV. SIMULATIONS

As described in the foreword, we can expect light enhancement in the groove. In order to evaluate the enhancement for the actual samples at different surface states, we carried out numerical simulations of the grating structure with trapezoid grooves [Fig. 4(a)] imitating the real nanograting induced by the 800-nm fs laser.

A. Simulation details

The numerical simulations were implemented by the finite difference time domain (FDTD) method[41] with a monochromatic plane wave of vertical incidence. At normal state, i.e., the irradiation fluence is far lower than the ablation threshold, we used the dielectric constant of graphite for the ordinary wave with a modified Lorentz-Drude model,[42] which can be expressed as

$$\varepsilon(\omega) = \varepsilon^{(f)}(\omega) + \varepsilon^{(b)}(\omega). \tag{1}$$

The intraband part $\varepsilon^{(f)}(\omega)$ is described by Drude mode

$$\varepsilon^{(f)}(\omega) = 1 - \frac{\Omega_p^2}{\omega(\omega + i\Gamma_0)}, \tag{2}$$

where $\Omega_p = \sqrt{f_0}\omega_p$, ω_p is the plasma frequency, f_0 is the oscillator strength, and Γ_0 is the damping constant.

The interband part $\varepsilon^{(b)}(\omega)$ is described by modified Lorentz mode

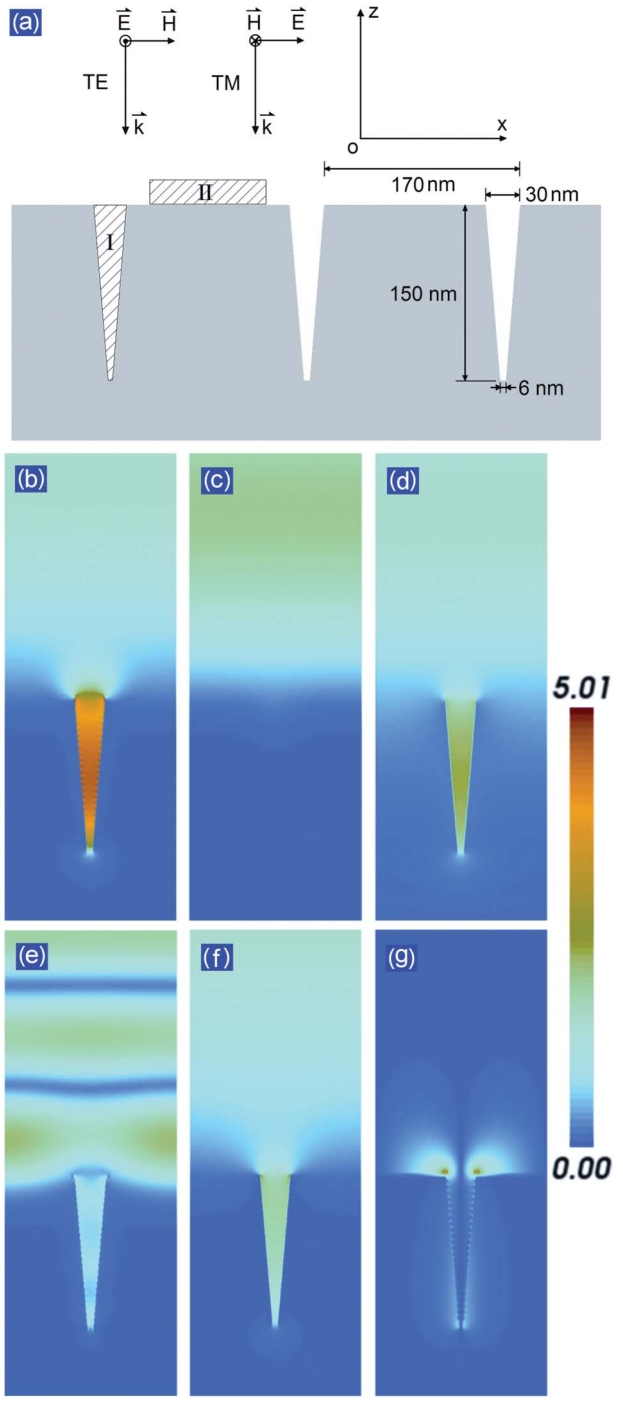

FIG. 4. (Color online) Simulations of the optical properties of the nanograting induced by 800-nm fs laser at normal and high-excited states. (a) A schematic view of the nanograting under study with the definition of different parameters involved. The diagonal areas I and II denote the groove and ridge areas for the average enhancement calculation, respectively. The field amplitude distributions under different irradiation conditions in one period (periodic boundary condition): (b) the E_x at the high-excited state with 800-nm TM wave; (c) the E_y at the high-excited state with 800-nm TE wave; (d) the E_x at the normal state with 800-nm TM wave; (e) the E_x at the high-excited state with 200-nm TM wave; (f) the E_x at the high-excited state with 2000-nm TM wave; and (g) the E_z at the high-excited state with 800-nm TM wave.

$$\varepsilon^{(b)}(\omega) = -\sum_{j=1}^{k} \frac{F_j}{(\omega^2 - \omega_j^2) + i\omega\Gamma_j'}, \tag{3}$$

where k is the number of employed oscillators, $F_j = f_j\omega_p^2$, and the frequency-dependent damping constant Γ_j' is expressed as

$$\Gamma_j' = \Gamma_j \exp\left[-\alpha_j\left(\frac{\hbar\omega - \hbar\omega_j}{\Gamma_j}\right)^2\right]. \tag{4}$$

The values of the fitting parameters Γ_j, ω_j, f_j, α_j, and other parameters are listed in Ref. 42.

At the state that the surface electrons are highly excited, i.e., the irradiation fluence is near the ablation threshold, we propose that the graphite surface has the optical properties similar to liquid carbon that behaves the metallic characteristic, and the dielectric constant is described with the Drude model, which is expressed as

$$\varepsilon_m(\omega) = \varepsilon_\infty - \frac{\omega_p^2}{\omega(\omega + i\Gamma)}, \tag{5}$$

where the parameters $\varepsilon_\infty = 2.726$, $\omega_p = 2.910 \times 10^{16}$ rad/s, and $\Gamma = 3.147 \times 10^{15}$ Hz are obtained by fitting to the parameters of liquid carbon[43] with ensuring the best fitting result in the wavelength range of our investigation.

B. Cavity-mode excitation

At the high-excited state, the amplitude distribution of E fields in one period under the irradiation of transverse-magnetic (TM) wave and transverse-electric (TE) wave of 800 nm is shown in Figs. 4(b) and 4(c). The polarization effect is prominent. The field in the groove is strongly enhanced in TM wave case, which is agreed with the characteristic of light transmission enhancement of subwavelength slit, for waveguide mode is only allowed for TM wave when the slit has a subwavelength width. In nature, this field enhancement of polarization sensitiveness in the nanostructures of high-excited surface should be a universal phenomenon. Consequently, we consider that this effect acts as an important feedback mechanism for the growth of nanogratings and the polarization dependence of nanograting orientation. In the following, we only discuss the TM wave case.

Figures 5(a) and 5(b) displays the average absolute and relative enhancement for the groove area, respectively [$\overline{|E_x^g|^2}/\overline{|E_0|^2}$ and $\overline{|E_x^g|^2}/\overline{|E_x^r|^2}$ and E_x^g and E_x^r are the electric fields in the groove and near the ridge surface, respectively, as the diagonal areas shown in Fig. 4(a)]. At the high-excited state, the two peaks located at about 800 and 355 nm are due to cavity-mode excitation. The high peak at about 800 nm is consistent with the laser wavelength used for our experiments. Comparing the amplitude distributions of E_x at wavelength of 800, 200, and 2000 nm [see Figs. 4(b), 4(e), and 4(f)], we can see that at the resonant wavelength, the E_x field is intensively enhanced and localized in groove area; the relative enhancement factor can be larger than 100. Nevertheless, at normal state we cannot observe resonant characteristic in this wavelength range [Figs. 5(a) and 5(b)], and the enhancement of E_x at 800 nm [Fig. 4(d)] is far lower than

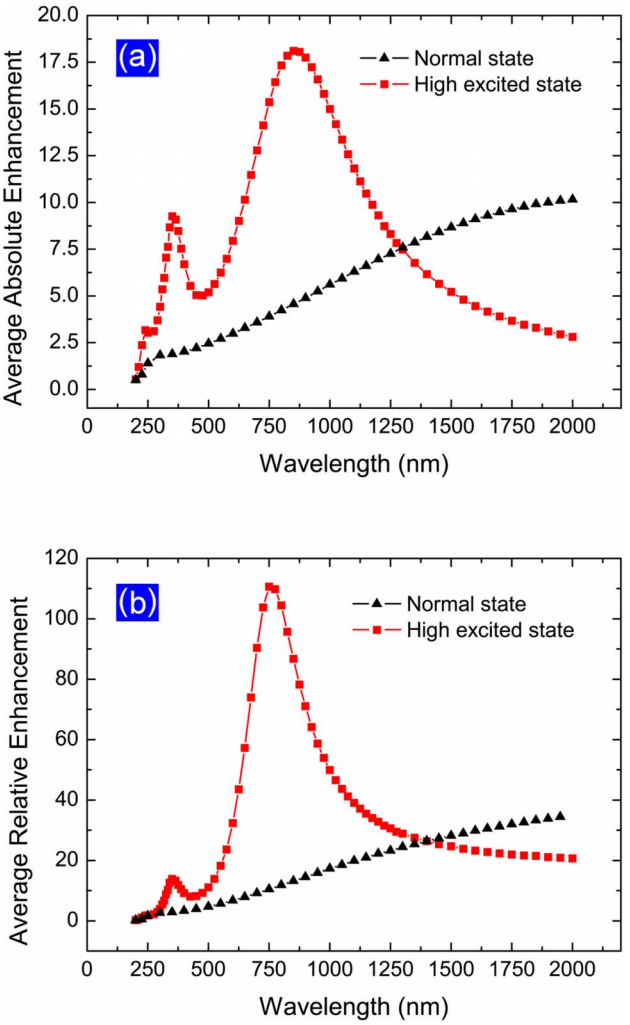

FIG. 5. (Color online) The average absolute (a) and relative (b) enhancements of E_x field in the groove for the normal and high-excited states in the wavelength range from ultraviolet to near infrared in the TM wave case.

that at the high-excited state. These results confirm our proposition that the optical properties of the high-excited state of materials determine the formation of laser-induced nanogratings. Based on this conclusion, it is easy to explain why the nanogratings on diamond and graphite have the same characteristics. Under laser irradiation with fluences near respective ablation thresholds, their surfaces present the same state similar to metallic liquid carbon. Furthermore, actually, such a high-excited state may be responsible for the similarity of laser-induced deep-subwavelength ripples in various materials[6–26] involving dielectrics, semiconductors, and metals with great different physical properties at normal state.

V. DISCUSSION

A. Origin of polarization dependence of nanogratings

As the simulation demonstrated, the strong polarization sensitiveness of field enhancement in the groove can explain the polarization dependence of nanograting orientation. Further, it means that once there are nanoscale apertures in the surface irradiated by a laser with the threshold fluence, the extraordinary field enhancement of polarization dependence will induce a positive feedback process for the groove formation. Whereas, we suggest that the cavity-mode excitation is an important factor rather than the lone reason for the origin of the polarization dependence of nanogratings[26] because the cavity mode, whose characteristic is mainly determined by the structural parameters of the cavity, is an extrinsic property for material and cannot spontaneously appear on a smooth surface. As a matter of fact, the laser-induced plasma influences the process of laser-matter interactions through a variety of different ways. It is well known that at the interface between a dielectric and a conductor, the coupling of the electromagnetic fields to oscillations of the electron plasma can support a highly confined surface electromagnetic wave called SP.[44] The SP is a solution of Maxwell equations that represents a TM wave propagating at the interface, so only TM-polarized light can excite SP. Thus, the polarization dependence of SP excitation may be another key factor, which is responsible for the initial polarization dependence of nanogratings.[26] Lately, the models of interferences between the light and plasma waves[25] and growth of nanoplasma[26] for the formation of planar nanostructures inside fused silica have been proposed. In addition, the mechanism of laser-induced microvoid is also suggested to be a plasma phenomenon.[45] In view of these studies, we consider that the surface or body nanoplasmons act an important role, especially at the initial stage, for the formation of nanogratings. The nanoplasmons can induce local-field enhancement and permanent structure changes[26,46] and grow with a feedback mechanism.[26,27] When the localized field-enhanced by nanoplasmons reaches the damage threshold, the nanoscale apertures, such as nanohole and nanogroove, will be produced via nanoscale explosions[47,48] or nanocrack.[26] For the TM characteristic between exciting light and plasmons, the orientation of plasmon-induced nanogroove is dependent on light polarization automatically. Once the nanoapertures are formed, the mechanism of extraordinary field enhancement via cavity-mode excitation will work, and the nanostructures will act as a seed for further ablation. Furthermore, the formed nanoapertures can act as a launcher for the SPs (Refs. 29–33, 44, and 49) and interact with SPs to form standing SP wave[50] for producing the initial grating profile via periodic energy deposition. Thus, the ablation process—groove deepening and expanding—will be more and more efficient by the self-fulfillment of resonant condition of cavity mode and standing SP wave, and the strong feedback of polarization sensitiveness of field enhancement in the groove. In short, in the nanograting formation, the initial polarization selection germs by the TM wave characteristic of plasmons and then reinforces by the cavity-mode excitation and standing SP wave formation.

B. Effect of surface roughness

Since surface nanostructures can induce high-localized field enhancement via exciting cavity mode and launching

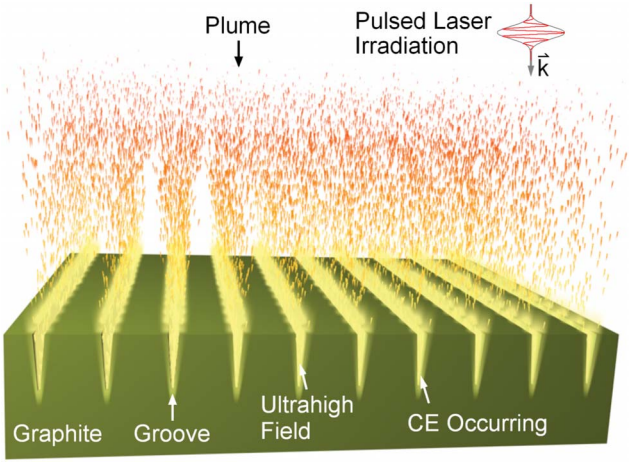

FIG. 6. (Color online) A schematic picture of CE occurring in the groove irradiated by ultrafast laser with the fluence near the ablation threshold.

SPs, we consider that the surface conditions of materials, such as surface roughness and stains that will induce localized field enhancement, have a crucial influence on the ablation. The effect that the surface roughening can reduce the threshold fluence for the formation of laser-induced fine ripple has been reported.[20] In our opinion, the cavity-mode-induced localized field enhancement in the surface nanoroughnesses is the most important cause for this effect.

C. Nanoscale Coulomb explosion in the groove

As the simulations exhibited, at the resonant wavelength, the light can be extraordinarily localized and enhanced in the groove. What will happen for such a high light intensity in such a small region and short-time scale? This question should be meaningful for us to understand the ablation mechanism for nanograting formation. Considering some aspects as follows, we propose that the nanoscale CE occurs in the groove under this condition, as the physical picture shown in Fig. 6. First, the occurrence of CE is dependent on the local charge density in an ultrashort time scale. Considering the fs timescale and localized ultrahigh field in the groove, we consider that this condition can induce CE. In detail, the ultrahigh field in the groove of nanoscale can activize an ultrafast localized photoionization and excite a mass of superhot surface electrons. Then the high-density electron ejections will induce localized transient surface charges, and abundant surface charges accumulating in an ultrashort time scale will build up of a strong electric field on the surface and bring on CE. Second, CE mechanism cannot only describe the ultrafast nonthermal formation of nanograting but also promote the understanding of CE experiments for bulk materials. To our knowledge, the investigations of CE in bulk materials are always based on the experiments in a macroscopical view;[51,52] the micromechanism of CE for bulk materials is not absolutely clear. How the localized transient surface charges occur and why the CE is prominent for the laser fluence near the ablation threshold ("gentle" phase[51]) are still problems for these investigations. From our investigation, these questions can be answered qualitatively. Owing to the strong localized fields in the nanoapertures as our simulations have shown, CE tends to occur localized in the surface nanoapertures,[10,51] which are prone to appear with the laser fluence near the ablation threshold (at higher fluence, the thermal effects will baffle the formation of nanostructures). Third, the abnormal phenomenon—high occurrence possibility of nanogratings on opaque graphite—can be understood by the CE mechanism. In our opinion, this especial property should relate to the high anisotropic physical properties of the plane graphite structure. The nonthermal ablation mechanisms of removal intact graphite sheets[48,53] and a burst of high-excited components[52] were observed and considered rooting in CE.[6,7,10,15,48,51] Due to the weak bonds between the planes, the surface charge density of graphite being able to ignite CE (Ref. 48) is approximately 1 order of magnitude lower than that of Si.[54] This low CE threshold property of graphite can explain why nanograting can be produced easily on graphite that is absolutely opaque to the incident laser. Since the occurrence of CE is dependent on the local charge density at short-time scale, the nonlinear processes, such as the multiphoton ionization, can enhance the nonlinear localized distribution of excited electrons and touch off CE more easily. For graphite, it has such a low CE threshold that it does not need very strong multiphoton nonlinear effect to induce CE. Therefore, the nanogratings can form in the opaque range of laser wavelength. In contrast, for the general materials with symmetrical physical properties, the higher CE threshold makes it hard to ignite CE by single-photon excitation. Therefore, strong multiphoton nonlinear effect, which is easier to occur in transparent materials under laser multiphoton irradiation with near-threshold fluence, is needed for these materials to ignite CE. This is a main reason why laser-induced nanostructures are prone to appear in wide band-gap materials ablated by near-infrared fs laser. Finally, the nanoscale CE occurring in the groove is responsible for the strong localized shock effect that induces the sheddings shown in Fig. 1(b).

VI. CONCLUSION

Our results indicate that the nanograting formation comes of interaction and intercrossing of a few physics fields. This investigation can give some insights to the phenomenon of laser-matter interactions. Above all, the formation of laser-induced nanogratings is not determined by the physical properties of materials at normal state but the high-excited state induced by ultrafast laser irradiation with the fluence near the ablation threshold. With this irradiation condition, in an ultrashort time scale, abundant electrons are excited and high-density plasmas are produced, which will change the surface physical properties greatly—especially the optical property. Such a change in optical properties will, in turn, intensively affect the laser-matter interactions by modulating the electromagnetic intensity distribution, inducing localized strong fields, and even arising CE in nanoscale as a result of exciting plentiful localized transient charges, which is responsible for the nonthermal ablation mechanism of ultrafast laser. This process is dominantly occurring in the intrinsic defects

or preformed nanostructures, especially the nanogroove for the cavity-mode enhancement of polarization dependence. Thus, via a positive feedback process, the polarization dependence nanograting will be formed. In addition, we propose that at the initial stage of nanograting formation, SPs act an important role for producing the seed nanoapertures and initial polarization dependence. Furthermore, the periodicity of the grating that cannot be obtained from the cavity mode may come from the standing SP mode. Nowadays, the theoretical work dealing with optical breakdown of diamond via first-principles electron dynamics has been reported.[39] Interestingly, their simulation shows that a coherent plasma oscillation persists for tens of femtoseconds, which may be meaningful for us to understand the dynamic process of laser-induced plasma and get some clues for the origin of nanogratings.

In short, we have demonstrated the experimental results of ultrafast laser-induced nanogratings on graphite and diamond, discussed the two main mechanisms for the polarization dependence of nanogratings—cavity mode and SP excitation, and described the picture of nanoscale CE occurring in the groove. This study can offer some insights for the exact physical mechanisms of laser-induced nanogratings and promote the understanding of ultrafast laser-matter interactions. On the other hand, the nanogratings on graphite and diamond might be of interest for the applications in nanophotonics or nanomechanics. In future, further experimental and theoretical investigations should be carried out to settle the outstanding issue: the origin of the periodicity of nanogratings.

ACKNOWLEDGMENTS

The authors are grateful to Yanfa Liu and Xueran Zeng for their support in the experiments. This work has been supported by grants from the Shanghai Institute of Optics and Fine Mechanics (SIOM), Chinese Academy of Sciences (CAS).

*syshm@163.com
†zzxu@mail.shcnc.ac.cn

[1] M. Birnbaum, J. Appl. Phys. **36**, 3688 (1965).
[2] D. C. Emmony, R. P. Howson, and L. J. Willis, Appl. Phys. Lett. **23**, 598 (1973).
[3] M. Oron and G. Sørensen, Appl. Phys. Lett. **35**, 782 (1979).
[4] J. E. Sipe, Jeff F. Young, J. S. Preston, and H. M. van Driel, Phys. Rev. B **27**, 1141 (1983); Jeff F. Young, J. S. Preston, H. M. van Driel, and J. E. Sipe, *ibid.* **27**, 1155 (1983).
[5] S. E. Clark and D. C. Emmony, Phys. Rev. B **40**, 2031 (1989).
[6] H. Varel, M. Wähmer, A. Rosenfeld, D. Ashkenasi, and E. E. B. Campbell, Appl. Surf. Sci. **127-129**, 128 (1998).
[7] M. Ozkan, A. P. Malshe, T. A. Railkar, W. D. Brown, M. D. Shirk, and P. A. Molian, Appl. Phys. Lett. **75**, 3716 (1999).
[8] J. Bonse, H. Sturm, D. Schmidt, and W. Kautek, Appl. Phys. A: Mater. Sci. Process. **71**, 657 (2000).
[9] J. Reif, F. Costache, M. Henyk, and S. V. Pandelov, Appl. Surf. Sci. **197-198**, 891 (2002).
[10] J. Reif, F. Costache, and M. Henyk, Proc. SPIE **4948**, 380 (2003); F. Costache, S. Kouteva-Arguirova, and J. Reif, Appl. Phys. A: Mater. Sci. Process. **79**, 1429 (2004); O. Varlamova, F. Costache, J. Reif, and M. Bestehorn, Appl. Surf. Sci. **252**, 4702 (2006).
[11] A. Borowiec and H. K. Haugen, Appl. Phys. Lett. **82**, 4462 (2003).
[12] Q. Wu, Y. Ma, R. Fang, Y. Liao, Q. Yu, X. Chen, and K. Wang, Appl. Phys. Lett. **82**, 1703 (2003).
[13] N. Yasumaru, K. Miyazaki, and J. Kiuchi, Appl. Phys. A: Mater. Sci. Process. **76**, 983 (2003).
[14] G. Daminelli, J. Krüger, and W. Kautek, Thin Solid Films **467**, 334 (2004).
[15] Y. Y. Dong and P. A. Molian, Appl. Phys. Lett. **84**, 10 (2004).
[16] W. Kautek, P. Rudolph, G. Daminelli, and J. Krüger, Appl. Phys. A: Mater. Sci. Process. **81**, 65 (2005).
[17] T. Q. Jia, H. X. Chen, M. Huang, F. L. Zhao, J. R. Qiu, R. X. Li, Z. Z. Xu, X. K. He, J. Zhang, and H. Kuroda, Phys. Rev. B **72**, 125429 (2005); T. Q. Jia, F. L. Zhao, M. Huang, H. X. Chen, J. R. Qiu, R. X. Li, Z. Z. Xu, and H. Kuroda, Appl. Phys. Lett. **88**, 111117 (2006).
[18] J. Bonse, M. Munz, and H. Sturm, J. Appl. Phys. **97**, 013538 (2005).
[19] R. Le Harzic, H. Schuck, D. Sauer, T. Anhut, I. Riemann, and K. König, Opt. Express **13**, 6651 (2005).
[20] T. Tomita, K. Kinoshita, S. Matsuo, and S. Hashimoto, Appl. Phys. Lett. **90**, 153115 (2007).
[21] G. Miyaji and K. Miyazaki, Appl. Phys. Lett. **91**, 123102 (2007).
[22] E. M. Hsu, T. H. R. Crawford, H. F. Tiedje, and H. K. Haugen, Appl. Phys. Lett. **91**, 111102 (2007).
[23] A. Weck, T. H. R. Crawford, D. S. Wilkinson, H. K. Haugen, and J. S. Preston, Appl. Phys. A: Mater. Sci. Process. **89**, 1001 (2007).
[24] M. Huang, F. L. Zhao, Y. Cheng, N. S. Xu, and Z. Z. Xu, Opt. Express **16**, 19354 (2008); M. Huang, F. L. Zhao, T. Q. Jia, Y. Cheng, N. S. Xu, and Z. Z. Xu, Nanotechnology **18**, 505301 (2007).
[25] Y. Shimotsuma, P. G. Kazansky, J. Qiu, and K. Hirao, Phys. Rev. Lett. **91**, 247405 (2003).
[26] V. R. Bhardwaj, E. Simova, P. P. Rajeev, C. Hnatovsky, R. S. Taylor, D. M. Rayner, and P. B. Corkum, Phys. Rev. Lett. **96**, 057404 (2006); P. P. Rajeev, M. Gertsvolf, C. Hnatovsky, E. Simova, R. S. Taylor, P. B. Corkum, D. M. Rayner, and V. R. Bhardwaj, J. Phys. B **40**, S273 (2007); R. Taylor, C. Hnatovsky, and E. Simova, Laser Photonics Rev. **2**, 26 (2008).
[27] P. P. Rajeev, M. Gertsvolf, E. Simova, C. Hnatovsky, R. S. Taylor, V. R. Bhardwaj, D. M. Rayner, and P. B. Corkum, Phys. Rev. Lett. **97**, 253001 (2006).
[28] T. W. Ebbesen, H. J. Lezec, H. F. Ghaemi, T. Thio, and P. A. Wolff, Nature (London) **391**, 667 (1998).
[29] W. L. Barnes, A. Dereux, and T. W. Ebbesen, Nature (London) **424**, 824 (2003).
[30] C. Genet and T. W. Ebbesen, Nature (London) **445**, 39 (2007).

[31] T. López-Rios, D. Mendoza, F. J. García-Vidal, J. Sánchez-Dehesa, and B. Pannetier, Phys. Rev. Lett. **81**, 665 (1998).
[32] J. A. Porto, F. J. García-Vidal, and J. B. Pendry, Phys. Rev. Lett. **83**, 2845 (1999).
[33] F. J. García-Vidal, H. J. Lezec, T. W. Ebbesen, and L. Martín-Moreno, Phys. Rev. Lett. **90**, 213901 (2003).
[34] J. Le Perchec, P. Quémerais, A. Barbara, and T. López-Ríos, Phys. Rev. Lett. **97**, 036405 (2006).
[35] M. M. Murnane, H. C. Kapteyn, and R. W. Falcone, Phys. Rev. Lett. **62**, 155 (1989).
[36] P. Audebert, Ph. Daguzan, A. Dos Santos, J. C. Gauthier, J. P. Geindre, S. Guizard, G. Hamoniaux, K. Krastev, P. Martin, G. Petite, and A. Antonetti, Phys. Rev. Lett. **73**, 1990 (1994).
[37] Q. Sun, H. Jiang, Y. Liu, Z. Wu, H. Yang, and Q. Gong, Opt. Lett. **30**, 320 (2005).
[38] J. Siegel, D. Puerto, W. Gawelda, G. Bachelier, J. Solis, L. Ehrentraut, and J. Bonse, Appl. Phys. Lett. **91**, 082902 (2007).
[39] T. Otobe, M. Yamagiwa, J.-I. Iwata, K. Yabana, T. Nakatsukasa, and G. F. Bertsch, Phys. Rev. B **77**, 165104 (2008).
[40] M. Huang, F. L. Zhao, Y. Cheng, N. S. Xu, and Z. Z. Xu (unpublished).
[41] E. M. Explorer, http://www.emexplorer.net
[42] A. B. Djurišić and E. Herbert Li, J. Appl. Phys. **85**, 7404 (1999).
[43] J. Steinbeck, G. Dresselhaus, and M. S. Dresselhaus, Int. J. Thermophys. **11**, 789 (1990).
[44] H. Raether, *Surface Plasmons on Smooth and Rough Surfaces and on Gratings* (Springer-Verlag, Berlin, 1988).
[45] H. Y. Sun, J. Song, C. B. Li, J. Xu, X. S. Wang, Y. Cheng, Z. Z. Xu, J. R. Qiu, and T. Q. Jia, Appl. Phys. A: Mater. Sci. Process. **88**, 285 (2007).
[46] L. N. Gaier, M. Lein, M. I. Stockman, P. L. Knight, P. B. Corkum, M. Yu Ivanov, and G. L. Yudin, J. Phys. B **37**, L57 (2004).
[47] E. N. Glezer and E. Mazur, Appl. Phys. Lett. **71**, 882 (1997).
[48] M. Lenner, A. Kaplan, and R. E. Palmer, Appl. Phys. Lett. **90**, 153119 (2007).
[49] E. Devaux, T. W. Ebbesen, J.-C. Weeber, and A. Dereux, Appl. Phys. Lett. **83**, 4936 (2003).
[50] H. Gao, J. Henzie, and T. W. Odom, Nano Lett. **6**, 2104 (2006).
[51] R. Stoian, A. Rosenfeld, D. Ashkenasi, I. V. Hertel, N. M. Bulgakova, and E. E. B. Campbell, Phys. Rev. Lett. **88**, 097603 (2002); R. Stoian, D. Ashkenasi, A. Rosenfeld, and E. E. B. Campbell, Phys. Rev. B **62**, 13167 (2000); D. Ashkenasi, R. Stoian, and A. Rosenfeld, Appl. Surf. Sci. **154-155**, 40 (2000).
[52] S. J. Henley, J. D. Carey, S. R. P. Silva, G. M. Fuge, M. N. R. Ashfold, and D. Anglos, Phys. Rev. B **72**, 205413 (2005).
[53] H. O. Jeschke, M. E. Garcia, and K. H. Bennemann, Phys. Rev. Lett. **87**, 015003 (2001).
[54] W. G. Roeterdink, L. B. F. Juurlink, O. P. H. Vaughan, J. D. Diez, M. Bonn, and A. W. Kleyn, Appl. Phys. Lett. **82**, 4190 (2003).